

Supporting Information

Cheng et al. 10.1073/pnas.1112998108

SI Materials and Methods

Transplant Model. We implemented two models of arterial grafting, a size-mismatch (heterotopic) and size-match (homotopic) approach. To stimulate remodeling, we intentionally performed heterotopic transplants (aorta to common carotid artery), as described (1, 2). Briefly, mice were anesthetized with ketamine/xylazine and exsanguinated with physiologic saline, and then a midline abdominal incision was made in the donor mice (euthanized) to expose the anterior thoracic cage and permit dissection of aorta, which was removed of perivascular adipose in situ. The donor aortae were washed with saline solution containing 100 U/mL heparin, and an 8-mm measured segment of the aorta was placed in physiologic saline on ice. The recipient mice (survival) were then anesthetized and dissected by a neck-line incision to expose the right common carotid artery. Two separate ligatures (<1 mm apart) using 9-0 silk suture were placed on the artery, and subsequently the common carotid artery was transected between the middle ties. The proximal and distal portions of the artery were passed through cuffs made of an autoclavable nylon tubing, 0.0155" in outside diameter and a 0.0135" inside diameter. The vessel and handle of the cuff were fixed by microhemostat clamps permitting excision of the previously placed ligatures. Each end of the transected common carotid artery segment was then everted over the cuff body and fixed to the cuff with an 11-0 silk suture. The donor aorta was removed from the ice and then implanted between the two ends of the carotid artery by sleeving the ends of the arterial segment over the artery cuff and ligating them with the 9-0 suture. The vascular clamps were removed, and evidence of pulsations was sought in both the grafted and native vessels. About 35 min were needed to perform the whole operation. To test if the response was caused by heterotopic placement or size mismatch of the artery, we also implemented a homotopic, size-match approach, where common carotid artery was grafted to common carotid artery, which caused no remodeling in control blood vessels.

Grafts were harvested 4 wk after transplant. Graft harvest was undertaken by exposure of the donor artery, followed by median sternotomy and left ventricular puncture and an infusion of a 0.9% NaCl solution at 4 °C. The donor carotid artery was then removed. The proximal half was placed in 4% phosphate-buffered formaldehyde (pH 7.2), and the distal half was placed in OTC medium (Triangle Biomedical Sciences) and rapidly frozen in liquid nitrogen. Five separate sections 10 μm apart were sectioned from different layers of the carotid artery. Sections were examined via a Sony 3CCD camera and television monitor and a Nikon microscope with images digitized with ImagePro analysis software (Media Cybernetics). The intima was defined as the region between the lumen and internal elastic lamina (IEL) and the media as the region between the internal and external elastic laminae.

Functional Studies in Isolated Aortic Arteries. Seven- to 10-wk-old (young) Bmal1-KO mice or age-matched littermate WT controls were anesthetized with ketamine/xylazine and subsequently exsanguinated. Residual blood was removed by perfusing physiologic saline by cardiac puncture. Untransplanted native aorta (control) and thoracic aortic grafts were isolated 4 wk after the transplant procedure. The control aorta and aortic graft were carefully dissected and cut into rings (2-mm thickness) for placement into organ chambers containing Krebs buffer main-

tained under physiologic conditions. The composition of Krebs-Henseleit solution (KHS; in mmol/L) was: NaCl 118.3, KCl 4.7, CaCl₂ 2.5, MgSO₄·7H₂O 1.2, KH₂PO₄ 1.2, NaHCO₃ 25, dextrose 5.6, and equilibrated with 95%O₂-5%CO₂ to maintain pH of 7.4 at 37 °C. The rings were suspended by two tungsten wires (25 μm diameter) and mounted in a vessel myograph system (6-mL chamber size; Multi Myograph; Danish Myo Technology). Isometric tension was measured by using a force transducer coupled to data acquisition system. A resting tension of 1.0 g was used throughout the experiments. After an equilibration period of 60 min (during which time KHS was changed every 10 min and the resting tension was readjusted), rings were precontracted with phenylephrine until a plateau was reached. Vessels were then washed with KHS, which was repeated at least three times to stabilize the tissue. Aortae were then precontracted with phenylephrine and concentration-dependent responses to the endothelium-dependent agonist, acetylcholine, and the endothelium-independent NO donor, sodium nitroprusside.

Histomorphometry. Four weeks posttransplantation, mice were anesthetized, exsanguinated, and perfused via the left ventricle with physiologic saline. Mice were subsequently perfusion fixed with neutral buffered formalin. Both control native aorta in the thoracic cavity and grafted aorta were carefully excised and postfixed either overnight for morphometric studies or immediately embedded in frozen medium for cryotome processing. Morphometric analysis of the large arteries was performed by using video microscopy as described. Perimeter (p) of the vessel lumen was taken as the circumference (C) of a circle and lumen diameter (D) determined from the equation $D = C/p$, assuming that the vessel cross-sections were circular in vivo. To determine thrombus area, the IEL and patent lumen were circumscribed to derive a radius (R) value from the formula $R = 2C/p$, and then IEL area and luminal area (A) were calculated by using the formula $A = \pi R^2$. Lesion/neointimal area was derived from the difference of IEL area and lumen area.

Real-Time PCR. RNA isolated by using RNA mini kits (Invitrogen) was reverse transcribed and subjected to real time PCR using 2-ΔΔCt method. For Bmal1 primers, both the forward and reverse primers were designed to bind within the mRNA regions coded by exons 4 and 5 that were disrupted by insertion of the neomycin-resistance gene cassette as described (3).

Primers used were as follows:

Mouse Perforin. F- GTGCCCAAGCCAGCGTCTCCA
R-AGGGGCTCCAGGCTGTAGTCCA

Mouse ICAM-2. F-GAGACGCCACGAATAAAATAATG
R-AGGGGACACCGTGCACCTAATGG

Mouse Granzyme-B. F-GGGGGCCCAACATCAAAGAA
R-CCCCAACCCAGCCACATAGCACA

Mouse CXCL-9. F-AGCCGAGGCACGATCCACTACA
R-TTTCCTCTTTTGTCTTTTCTT

Mouse Bmal1. F-ATGCAATGTCCAGGAAGTTAGATA
R-AATTAGGTGTTTCAGTTCGCAT

Mouse 18S. F- CGGCGCCCCCTCGATGCTCTTA
R- CCCCCGGCCGTCCCTCTTA

Immunohistochemistry. Standard frozen sectioning and immunohistochemistry was performed by using the ABC kit (Vector) using antibodies for cd68 (rat; Acris Antibodies; 1:50), cd3 (rabbit; Novus Biologicals; 1:100), and F4/80 (rat; BD Biosciences; 1:1,000).

1. Dietrich H, et al. (2000) Mouse model of transplant arteriosclerosis: Role of intercellular adhesion molecule-1. *Arterioscler Thromb Vasc Biol* 20:343–352.
2. Tereb DA, et al. (2001) Human T cells infiltrate and injure pig coronary artery grafts with activated but not quiescent endothelium in immunodeficient mouse hosts. *Transplantation* 71:1622–1630.

3. Bunger MK, et al. (2000) Mop3 is an essential component of the master circadian pacemaker in mammals. *Cell* 103:1009–1017.

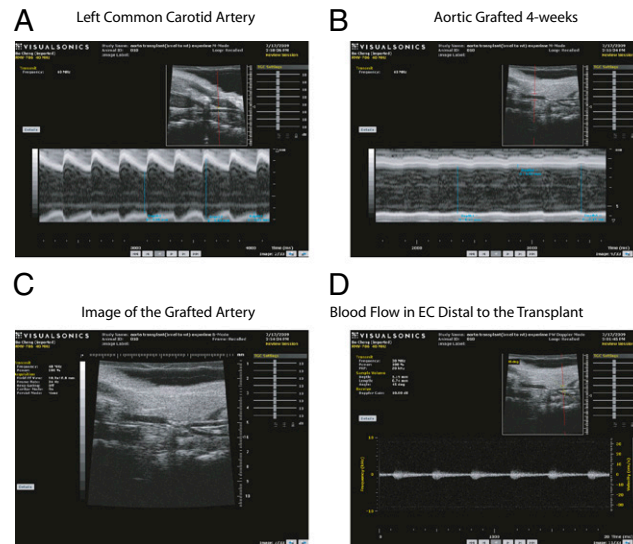


Fig. S1. Ultrasound imaging of aortic to common carotid artery anastomoses. Four weeks after transplantation, mice were anesthetized, and the arterial neck circulation was visualized noninvasively by using Vevo 770 ultrasound. Live imaging of the pulse wave form caused by flowing blood revealed robust systolic/diastolic deflections in the left common carotid artery wall (A), while deflections in the grafted aorta were blunted (B), which may reflect a difference in elasticity due to the enhanced wall thickness and native anatomical differences between the common carotid and aortic arteries. (C) Four weeks posttransplant, the graft is clearly patent, as is the bifurcation of the external and internal carotid artery, which was confirmed by flow velocity (D) in the external carotid artery, confirming the presence of a live, viable graft with flowing blood.

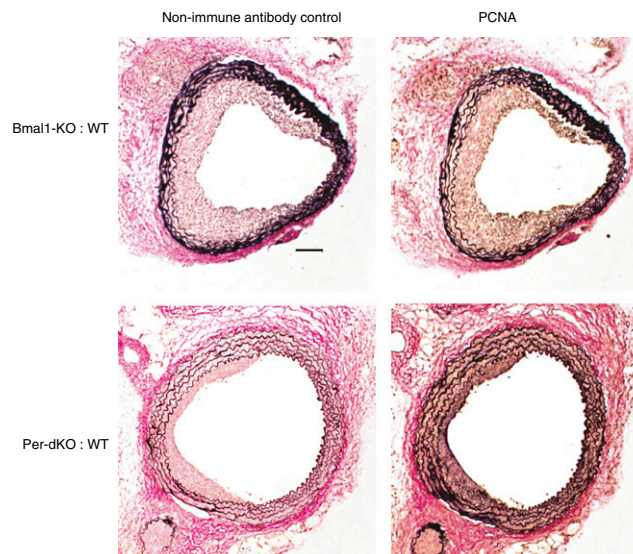


Fig. S2. Increased PCNA staining in circadian clock mutant transplants. Immunohistochemistry of aortic grafts in *Bmal1-KO:WT* and *Per-dKO:WT* mice revealed increased PCNA staining that was prominent within the lesion. There was no staining in nonimmune IgG controls.

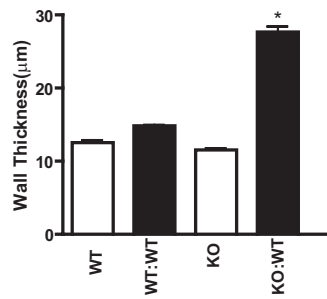


Fig. S3. Homotopic transplant does not alter lumen diameter. Changes in lumen diameter and wall thickness are an index of common carotid artery remodeling. Common carotid artery to common carotid artery transplants (homotopic) revealed no changes in lumen diameter 4 wk after transplantation in WT:WT and in Bmal1-KO to WT grafts ($n = 8$, WT:WT; $n = 8$, Bmal1-KO:WT). Importantly, this demonstrated that the size-matching approach caused no hemodynamic changes that might serve as a stimulus for remodeling in WT:WT and Bmal1-KO:WT grafts.

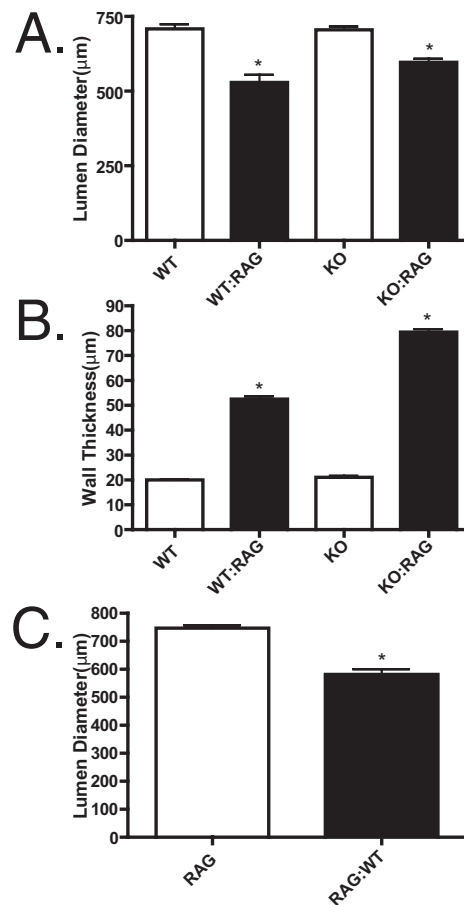


Fig. S4. Arteriosclerosis persists in Bmal1-KO:RAG1-KO mice but is absent in RAG1-KO:WT mice. Using the size-mismatch model (aorta:common carotid artery), lumen diameter of aortic grafts remodeled to comparable increments between Bmal1-KO:WT mice and Bmal1-KO:RAG-KO mice. There was a significant difference in increment of remodeling between the WT:RAG-1-KO and Bmal1-KO:RAG-1-KO, indexed as lumen diameter (A) and wall thickness (B) ($n = 6$, WT; $n = 6$, Bmal1-KO; $n = 6$, WT:RAG-1-KO; $n = 6$, Bmal1-KO:RAG-1-KO; $*P < 0.05$). (C) To test if arteriosclerotic lesion was pervasive among random gene mutant donors, we used donor aortic segments from RAG-1-KO mice and grafted to recipient WT mice. Although their diameter was reduced in RAG-KO grafts versus the native aorta, there was no neointimal formation/lesion in RAG-1-KO:WT mice ($n = 6$, RAG-1-KO; $n = 6$, RAG-1-KO:WT; $*P < 0.05$).